Iranian Journal of Chemical Engineering
Vol. 12, No. 2 (Spring 2015), IAChE

Adsorption Behavior of Short Alkyl Chain Imidazolium Ionic Liquidsat N-Butyl Acetate + Water Interface: Experiments and Modeling

J. Saien*, M. Kharazi, S. Asadabadi

Bu–Ali Sina University, Hamedan, Iran

Abstract

The adsorption behavior of three amphiphilic ionic liquids (ILs), 1-alkyl-3-methylimidazolium chloride {[Cnmim][Cl], n=6–8}at the interface of n-butyl acetate + water system was studied with IL concentration range of 1.00×10^{-4}-1.00×10^{-1} mol·dm^{-3} and temperature range of 293.2-318.2 K. The ILs behave as strong surfactants in this chemical system and significantly reduce the interfacial tension with the order of their alkyl chain length and is consistent with their hydrophobicity nature. An almost linear decrease of interfacial tension with temperature was also relevant. The experimental data were satisfactorily reproduced with Szyszkowski equation, implying an ideal ILs adsorption. In this regard, the Langmuir maximum interface excess and equilibrium adsorption constant were obtained at different temperatures for each IL. Accordingly, effectiveness of adsorption and adsorption tendency increase with the alkyl chain length. At the saturated interface, increasing temperature leads to declining Langmuir maximum interface excess due to disrupting surrounding water molecules around ILs hydrophobic portions. However, adsorption tendency of ILs increases slightly with temperature.

Keywords: *Ionic Liquids, Alkyl Chain Length, Interfacial Tension, Szyszkows kiequation, Ideal Adsorption*

1. Introduction

Ionic liquids (ILs) are entirely composed of ions and possess low melting points [1]. The unique physico-chemical properties of ILs such as very low vapor pressure, non-flammability, high thermal stability and ion conductivity have attracted much interest in recent years [2,3]. The ILs properties can be improved by modifying cations and/or anions. Accordingly, ILs have been utilized in many fields such as catalyzing reactions [4], corrosion inhibition [5], gas–liquid absorption[6], liquid membrane separation [7], liquid–liquid extraction [8] and electrochemistry [9].

One of the marvelous characteristics of ILs is surface/interface activity due to their amphiphilic nature just like conventional surfactants [10,11]. However, most studies have focused on ILs behavior as surfactants in aqueous phases. For instance, Zhao [12]. synthesized n-alkyl-n-methyl piperidinium

bromide ILs and studied their micelle formation and surface activity in aqueous solutions. It was shown that by increasing alkyl chain length, critical micelle concentration (CMC) decreases; however, adsorption efficiency and maximum surface excess rise with increasing hydrophobicity of ILs. Among different kinds of ILs, imidazolium-based ones have been conventionally considered due to their excellent surface activity [3,5]. In this regard, as shown in Fig. 1: a typical imidazolium-based IL possesses cationic hydrophilic (head group) and hydrophobic (tail) portions, providing a high tendency to adsorb at the surface of solutions. Matsubara *et al*. [13], for instance, studied the surface tension of aqueous solutions containing imidazolium ILs at different temperatures and demonstrated that reduction in surface tension occurs with temperature.

There are, however, few literature reports exist that deal with the adsorption of ILs at the oil-water interface and interfacial tension (IFT) variations, despite the significant role of this property in mass transfer phenomenon [14]. Our previous study was focused on the IFT variation and micelle formation of imidazolium-based ILs at toluene + water system [15]. The used ILs significantly reduced the IFT and the adsorption tendency revealed increasing with temperature. Considering the chemical structure of n-butyl acetate and from adsorption point of view, different results are expected with this chemical system.

The aim of present work was to study the adsorption behavior of three conventional imidazolium-based chloride ILs, namely 1-hexyl-3-methylimidazolium chloride, 1-heptyl-3-methylimidazolium chloride and 1-octyl-3-methylimidazolium chloride {briefly: ($[C_n mim][Cl]$, n=6, 7 and 8)} at n-butyl acetate + water interface. This chemical system has been recommended by the EFCE working party [16] as a system with moderate IFT (about 14 $mN \cdot m^{-1}$) for liquid–liquid extraction studies and has been frequently used in different studies [17-20]. An ILs concentration range of 1.00×10^{-4}-1.00×10^{-1} mol/L and temperature range of 293.2- 318.2 K were utilized. The Szyszkowski equation was then employed to correlate the experimental data in relation to ILs bulk concentrations. Accordingly, related parameters of interface activity were obtained and discussed.

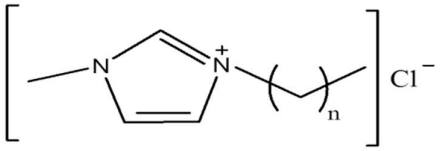

Figure 1. The chemical structure of 1-alkyl-3-methylimidazolium chloride.

2. Experimental

2-1. Materials

N-butyl acetate with mass fraction purity of more than 0.995 was purchased from Merck. The raw materials for synthesizing and purifying ILs, including: 1-methylimidazole, 1-chlorohexane, 1-chloroheptane, 1-chlorooctane and ethyl acetate were also purchased from Merck and Riedel-de Haen with mass fraction purity of more than 0.999, 0.99,0.98, 0.96 and 0.995, respectively. All materials were used without further purification. Fresh deionized water with electrical conductivity of 0.07 $\mu S \cdot cm^{-1}$ was used for aqueous solutions throughout the

experiments. The specifications of the used chemicals are given in Table 1. Each of the ILs, [C_6mim][Cl], [C_7mim][Cl] and [C_8mim][Cl], was prepared according to a standard method [21,22] and details have been described in our previous study [15]. Synthesized ILs were characterized by the way of ^{1}H NMR, ^{13}C NMR and mass spectroscopy, the characterization data were in agreement with the expected structure. The purity was confirmed by the appearance of just the ILs peaks and none for reactants and/or by-products.

Table 1
Origin and mass fraction purity of the used materials.

Chemical Name	Origin	Purity
n-butyl acetate	Merck	> 0.995
1-methylimidazole	Merck	> 0.999
1-chlorohexane	Merck	> 0.99
1-chloroheptane	Merck	> 0.98
1-chlorooctane	Riedel-de Haen	> 0.96
ethyl acetate	Merck	> 0.995

2-2. IFT measurements

The drop volume method was used to measure the IFT values. It is a reproducible technique and has been used by other investigators [13,23]. The details of drop-forming device and the procedure are reported in previous studies [24,25]. In this method, IFT, γ, is obtained from the following equation [26].

$$\gamma = \frac{V \Delta \rho g}{r} \varphi\left(\frac{r}{\sqrt[3]{V}}\right) \qquad (1)$$

where V is drop volume falling off a capillary into the organic phase; $\Delta\rho$ is the density difference between the aqueous and organic liquids (ρ_w and ρ_o), g and r are the acceleration of gravity and capillary radius (0.35 mm in this study), respectively, and $\varphi\left(r/\sqrt[3]{V}\right)$ is a constant which can be obtained from empirical relations [23].

The contacting media and conducting tube to a capillary were temperature adjusted at desired temperature, using a calibrated thermostat (OPTIMA 740, Japan) with an uncertainty of ± 0.1 K.

IL aqueous solutions were prepared by mass using an Ohaus (Adventurer Pro, AV 264) balance with an uncertainty of ±0.1 mg. Also, 200 and 250 (±0.2) cm^3 volumetric flasks and 5 and 10 (±0.01 and ±0.02) cm^3 volumetric pipettes were used. Different ILs concentrations from 1.0×10^{-4} to 1.0×10^{-1} mol·dm^{-3} were prepared and examined. The absolute maximum standard deviation of concentrations was $\pm\ 0.01\times10^{-3}$ mol/L for all cases. Each IL concentration was utilized for IFT measurements at different temperatures from 293.2 to 318.2 K.

Prior to experiments, equal volumes of both phases (100 cm^3) with corresponding aqueous phase concentrations of the ILs were mixed for at least 30 minutes, and then left to rest for another 30 minutes. It is notable that the mutual solubility of organic and aqueous phases was very low and that the formation of emulsion of either phase in another was not observed. Samples of the organic and the aqueous phases were also withdrawn to measure their density at different temperatures. Density was measured by means of an oscillating U-tube densimeter (Anton Paar DMA4500, Austria), provided with automatic viscosity correction. The uncertainty for density measurements was

±0.01 kg·m^{-3}. The estimated average uncertainty for all the measured IFT data was ±0.1 mN·m^{-1}.

To examine the performance and the reliability of the method, the IFT of the pure chemical system of n-butyl acetate + water (binary saturated, without IL) at 298.2 K was compared with reported values in the literature. The obtained value of 14.0mN·m^{-1} is in agreement with reported values of 14.1 and 14.4mN·m^{-1} [27,28].

3. Results and discussion

3-1. Experimental results

A concentration range of ILs from very low to about the CMC was utilized, each at six temperatures, ranging from 293.2 to 318.2 K. Density of individual IL solutions changed with both concentration and temperature. The aqueous and organic phase densities varied within 990.33 to 998.25 kg·m^{-3} and 856.32 to 882.44 kg·m^{-3}, respectively.

To ensure the attainment of equilibrium condition, the IFT changes with drop formation time, obtained with different aqueous phase flow rates from 0.0005 to 0.005 cm^3·s^{-1} were measured. The results with typical ILs concentration of 5.0×10^{-3} mol/L at 298.2 K are presented in Fig. 2. This figure demonstrates that the used ILs have no adequate time to adsorb at the interface when drop formation is fast. Therefore, the dynamic IFT is related to short times of drop formation (less than about 40 s here). As the formation time increases, each IL has a greater chance to accumulate at the interface. Eventually, when the time of drop formation becomes sufficiently long, the interface expansion occurs adequately slow to find equilibrium adsorption and no meaningful change is relevant with more drop formation times.

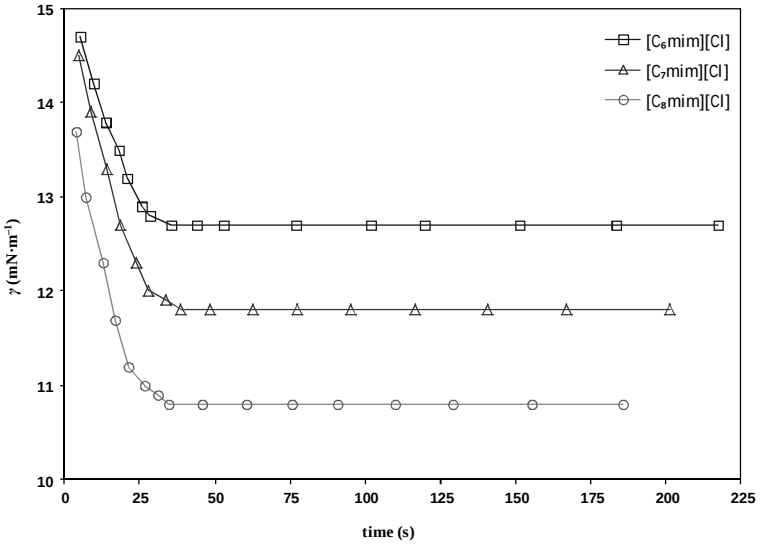

Figure 2. IFT variation as a function of drop formation time for ILs at typical concentration of 5.00×10^{-3} mol/L and temperature of 298.2 K.

The IFT data and phase densities at different temperatures as well as IL concentrations are given in the supplementary material. The measured IFT values were within the range of 13.4 to 14.0 mN·m^{-1} for the pure system (at different

temperatures, without any IL), 11.3 to 13.2 $mN{\cdot}m^{-1}$ with [C_6mim][Cl], 10.4 to 12.4 $mN{\cdot}m^{-1}$with [C_7mim][Cl] and 9.4 to 11.3 $mN{\cdot}m^{-1}$ with [C_8mim][Cl]. The average percentages of the IFT decrease were 20.2, 26.2 and 33.1%, respectively.

In Fig. 3, the IFT variations versus ILs concentration at different temperatures are presented. As can be seen, IFT significantly decreases with low amounts of the ILs (to about 1.00×10^{-2} mol/L) and then varies slowly by approaching CMC. Because of their amphiphilic nature, ILs just like conventional surfactants migrate toward the interface and by increasing their concentration more adsorption occurs, leading to further decrease in the IFT [29]. The interfacial activity of the used ILs appear in the order of [C_8mim][Cl]> [C_7mim][Cl] >[C_6mim][Cl]. As expected, more methylene groups (–CH_2–) in the ILs structure causes IFT to decrease more due to the greater hydrophobic nature in their tail [30]. Finally, IFT decreases almost linearly with temperature for each of the ILs concentration (Fig. 4). Rising temperature causes the kinetic of the molecules to improve and consequently, IFT diminishes [13].

3-2. Theoretical modeling

In most studies, Gibbs [31], Langmuir [32], Szyszkowski [33] and Frumkin [34] adsorption equations have been employed to relate interface adsorption and bulk concentration of surfactants and ILs. Among them, the Szyszkowski equation [35] gives the best fit with the obtained data here:

$$\gamma = \gamma_0 - 2RT\Gamma_m \ln(1 + K_L C_{IL}) \qquad (2)$$

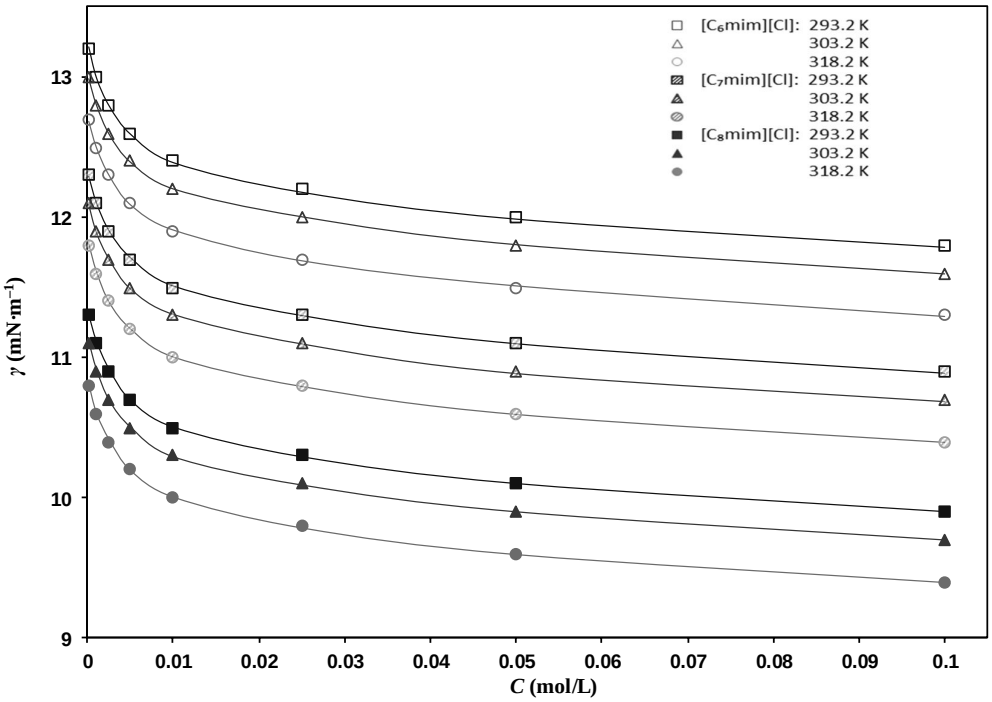

Figure 3. IFT variation as a function of ILs concentration at different temperatures. Solid lines correspond to theoretical curves obtained by the Szyszkowski model.

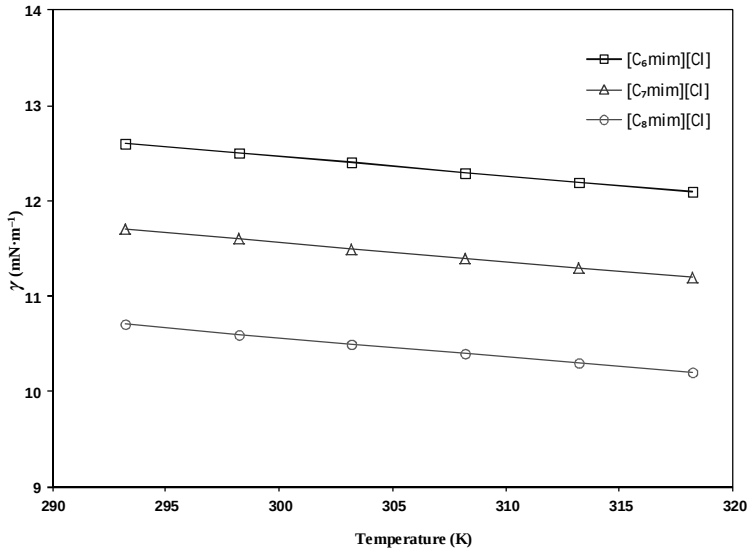

Figure 4. IFT variation as a function of temperature in the presence of ILs at typical concentration of 5.00×10^{-3} mol/L.

where γ_0 is the IFT of pure chemical system (C_{IL}=0); R and T are gas law constant and absolute temperature; C_{IL}, Γ_m and K_L are the IL bulk concentration, maximum interfacial concentration (under saturated interface) and the Langmuir equilibrium adsorption constant, respectively. In a simple convention, the factor 2 stands for the dissociation of each ionic surface active substance into its cation and anion.

The coefficient of determination, R^2, which is the difference between calculated and experimental IFT values, was obtained by [36]:

$$R^2 = 1 - \frac{\sum_{i=1}^{N} (\gamma_{cal,i} - \gamma_{exp,i})^2}{\sum_{i=1}^{N} (\bar{\gamma} - \gamma_{exp,i})^2} \qquad (3)$$

where N, γ_{cal}, γ_{exp} and $\bar{\gamma}$ are the number of data used in the fitting, the IFT calculated by the model, the experimental IFT and the average of all the appropriate experimental values, respectively. The corresponding R^2 values (within 0.9720 - 0.9990) are listed in Table 2 and indicate consistent fitting with the model. In Fig. 3, solid lines are theoretical curves, obtained based on Szyszkowski equation.

In our previous study [15], non-ideal interaction, mainly electrostatic repulsion, between adsorbed ILs was relevant at toluene + water interface. However, an ideal monolayer adsorption can be concluded here from the agreement with Szyszkowski equation [37]. Different adsorption behavior can be attributed to the interaction between ILs molecules with both organic and aqueous phase molecules. Considering the structure of the used ILs (Fig. 1), it is clear that there is acidic hydrogen on carbon number 2 (between two electronegative nitrogen atoms). There is, therefore, high possibility of hydrogen bonding between the acidic

Table 2
Minimum area occupied by a molecule, A_m, standard free energy of adsorption, ΔG°_{ads}, and coefficient of determination, R^2, for adsorption of ILs at different temperatures.

T (K)	$A_m \times 10^{18}$ (m^2)	$-\Delta G^{\circ}_{ads}$ ($kJ \cdot mol^{-1}$)	R^2
	[C_6mim][Cl]		
293.2	0.106	162.58	0.9999
298.2	0.108	165.87	0.9996
303.2	0.109	169.69	0.9998
308.2	0.111	173.51	0.9994
313.2	0.113	177.37	0.9997
318.2	0.130	181.24	0.9998
	[C_7mim][Cl]		
293.2	0.096	201.80	0.9868
298.2	0.098	205.93	0.9865
303.2	0.099	210.07	0.9869
308.2	0.101	214.22	0.9866
313.2	0.103	218.49	0.9864
318.2	0.118	222.78	0.9868
	[C_8mim][Cl]		
293.2	0.090	235.63	0.9726
298.2	0.092	240.13	0.9728
303.2	0.093	244.76	0.9727
308.2	0.095	249.41	0.9729
313.2	0.096	254.14	0.9728
318.2	0.111	258.93	0.9727

hydrogen and electronegative atoms in both n-butyl acetate and water molecules. This interaction decreases or diminishes repulsions between adsorbed ILs molecules at the interface, causing the ideal adsorption behavior in this chemical system.

Based on the Gibbs adsorption theory and by using the slope of the IFT plots versus C_{IL} (Fig. 3), interface excess, Γ, was obtained for each IL from [37]:

$$\Gamma = -\frac{C_{IL}}{2RT}\left(\frac{d\gamma}{dC_{IL}}\right) \quad (4)$$

The interface excess variation as a function of ILs concentration is presented in Fig. 5. The trends clearly demonstrate forming monolayer adsorption since the interface excess rises sharply at low concentration and then a plateau appears. For concentrations below but near the CMC, the interface excess tends to constant values corresponding to the maximum interface excess (Γ_m). Estimated Γ_m values from Eq. 4 and Fig. 5 are approximately the same as those obtained from fitting by Szyszkowski equation. Relevantly, the obtained maximum interface excess (from fitting) for each IL is depicted in Fig. 6. By increasing temperature, Γ_m decreases due to disrupting surrounding water molecules around hydrophobic portion which leads to less transference of ILs toward the interface [38]. It is also reasonable to attain higher Γ_m value by [C_8mim][Cl] than by [C_7mim][Cl] and [C_6mim][Cl], since higher methylene group (–CH_2–) in the ILs tail provides higher hydrophobicity, which in turn gives higher adsorption effectiveness, Γ_m values [30].

Corresponding to Γ_m, the minimum area occupied by an adsorbed molecule at the interface, A_m, can be obtained from the following equation [39]:

$$A_m = \frac{1}{\Gamma_m N_{Av}} \quad (5)$$

in which N_{Av} is the Avogadro's number. The calculated A_m values for each IL at different temperatures are also listed in Table 2. When concentration at the interface decreases, each molecule occupies more area.

The adsorption tendency is characterized by the Langmuir adsorption constant, K_L, for which the variation with temperature is

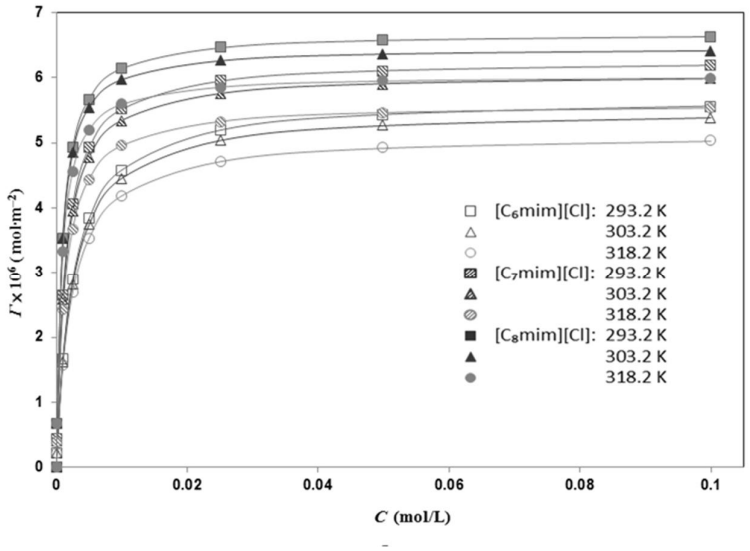

Figure 5. Interface excess as a function of ILs concentration at different temperatures.

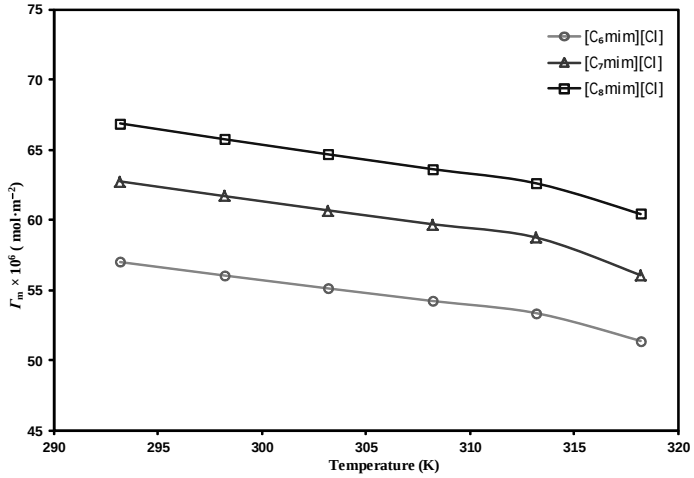

Figure 6. Maximum interface excess as a function of temperature for the used ILs.

shown in Fig. 7. As can be seen, temperature has a slight effect on the Langmuir adsorption constant. What is more, adsorption tendency increases with alkyl chain length. Longer chain ILs exhibit higher adsorption tendency due to their higher hydrophobicity.

Another important parameter, relevant to equilibrium constant is standard free energy of adsorption, ΔG°_{ads}, which is calculated from [38]:

$$\Delta G^{\circ}_{ads} = -2RT \ln\left(\frac{K_L \rho'}{2}\right) \quad (6)$$

Where ρ' $(\rho' = \rho_w/18)$ is molar concentration of water at a given temperature. Corresponding standard free energy of adsorption of ILs at different temperatures are given in Table 2. From negative values of ΔG°_{ads}, it can easily be concluded that ILs adsorption is spontaneous in all cases.

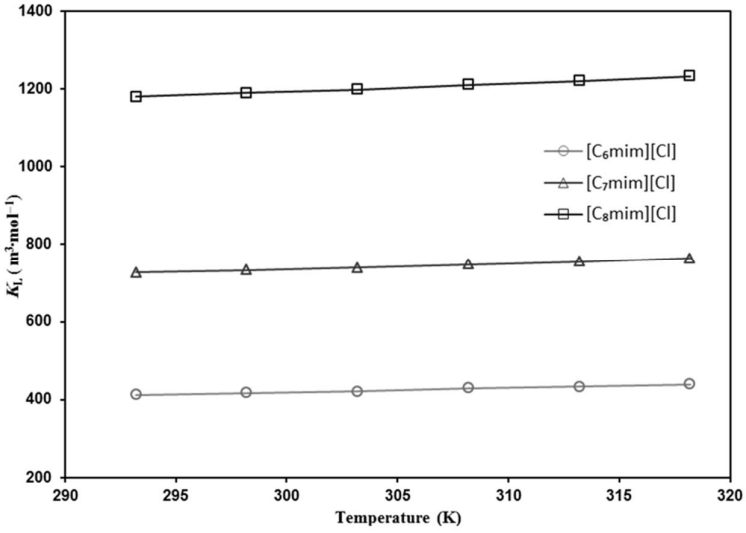

Figure 7. Equilibrium adsorption constant as a function of temperature for the used ILs.

4. Conclusions

The amphiphilic imidazolioum-based ILs, [C_6mim][Cl], [C_7mim][Cl] and [C_8mim][Cl], significantly reduce the interfacial tension of n-butyl acetate + water system at different temperatures. The average percentages of IFT decrease were 20.2, 26.2 and 33.1%, respectively, within the applied range of temperature.

Studied interfacial properties of the ILs were distinctive with respect to hydrophobicity feature relevant to alkyl chain length in their molecular structure. In all cases, an almost linear decrease of IFT with temperature was relevant.

The experimental data were satisfactorily reproduced with the Szyszkowski adsorption equation, indicating an ideal monolayer adsorption behavior due to the chemical nature of the ILs in contact with organic and aqueous phases. Accordingly, saturated interface excess decreases with rising temperature; however, increases with hydrophobic nature of ILs. In the meantime, the alkyl chain length shows greater influence on the Langmuir adsorption constant than temperature.

The results illuminate the capability of the used ionic liquids in decreasing the interfacial tension of "n-butyl acetate + water" system and therefore altering hydrodynamic and mass transfer in processes like liquid–liquid extraction. The remaining major problems to be investigated are the behavior of similar structure long chain ionic liquids as well as the influence of real aqueous phase pH and the extent of salinity.

Acknowledgments

The authors wish to acknowledge the university authorities for providing the financial support to carry out this work.

Supplementary material

The supplementary material associated with this article can be found in the online version, (see Table at the end of this manuscript)

Supplementary Table

Ionic Liquid Concentration, C_{IL}, Phase Densities, ρ , Drop Formation Time, t, and IFT Values, γ, for Each IL at Different Temperatures [a]

T(K)	C_{IL} (mol·dm^{-3})	ρ_w (kg·m^{-3})	ρ_o (kg·m^{-3})	t (s)	γ (mN·m^{1})
		[C_6mim][Cl]			
293.2	$1.00\cdot10^{-4}$	998.23	882.40	162	13.2
	$1.00\cdot10^{-3}$	998.23	882.40	157	13.0
	$2.50\cdot10^{-3}$	998.24	882.40	152	12.8
	$5.00\cdot10^{-3}$	998.35	882.40	146	12.6
	$1.00\cdot10^{-2}$	998.38	882.40	141	12.4
	$2.50\cdot10^{-2}$	998.41	882.40	136	12.2
	$5.00\cdot10^{-2}$	998.67	882.40	130	12.0
	$1.00\cdot10^{-1}$	998.80	882.40	125	11.8
298.2	$1.00\cdot10^{-4}$	997.06	877.23	154	13.1
	$1.00\cdot10^{-3}$	997.07	877.23	149	12.9
	$2.50\cdot10^{-3}$	997.09	877.23	144	12.7
	$5.00\cdot10^{-3}$	997.16	877.23	140	12.5
	$1.00\cdot10^{-2}$	997.20	877.23	135	12.3
	$2.50\cdot10^{-2}$	997.25	877.23	131	12.1
	$5.00\cdot10^{-2}$	997.51	877.23	126	11.9
	$1.00\cdot10^{-1}$	997.67	877.23	122	11.7
303.2	$1.00\cdot10^{-4}$	995.64	872.04	147	13.0
	$1.00\cdot10^{-3}$	995.64	872.04	143	12.8
	$2.50\cdot10^{-3}$	995.73	872.04	138	12.6
	$5.00\cdot10^{-3}$	995.79	872.04	133	12.4
	$1.00\cdot10^{-2}$	995.87	872.04	129	12.2
	$2.50\cdot10^{-2}$	996.14	872.04	124	12.0
	$5.00\cdot10^{-2}$	996.29	872.04	120	11.8
	$1.00\cdot10^{-1}$	996.41	872.04	116	11.6
308.2	$1.00\cdot10^{-4}$	994.04	866.83	140	12.9
	$1.00\cdot10^{-3}$	994.05	866.83	136	12.7
	$2.50\cdot10^{-3}$	994.15	866.83	132	12.5
	$5.00\cdot10^{-3}$	994.20	866.83	127	12.3
	$1.00\cdot10^{-2}$	994.28	866.83	122	12.1
	$2.50\cdot10^{-2}$	994.56	866.83	118	11.9
	$5.00\cdot10^{-2}$	994.76	866.83	113	11.7
	$1.00\cdot10^{-1}$	994.90	866.83	108	11.5
313.2	$1.00\cdot10^{-4}$	992.14	861.59	132	12.8
	$1.00\cdot10^{-3}$	992.29	861.59	127	12.6

	$2.50\cdot10^{-3}$	992.41	861.59	122	12.4
***T*(K)**	C_{IL} **(mol·dm^{-3})**	ρ_w **(kg·m^{-3})**	ρ_o **(kg·m^{-3})**	t **(s)**	γ **(mN·m^{-1})**
	$5.00\cdot10^{-3}$	992.68	861.59	117	12.2
	$1.00\cdot10^{-2}$	992.86	861.59	113	12.0
	$2.50\cdot10^{-2}$	993.00	861.59	109	11.8
	$5.00\cdot10^{-2}$	993.14	861.59	105	11.6
	$1.00\cdot10^{-1}$	993.44	861.59	100	11.4
318.2	$1.00\cdot10^{-4}$	991.04	856.32	124	12.7
	$1.00\cdot10^{-3}$	991.05	856.32	120	12.5
	$2.50\cdot10^{-3}$	991.15	856.32	116	12.3
	$5.00\cdot10^{-3}$	991.20	856.32	111	12.1
	$1.00\cdot10^{-2}$	991.28	856.32	106	11.9
	$2.50\cdot10^{-2}$	991.56	856.32	101	11.7
	$5.00\cdot10^{-2}$	991.76	856.32	96	11.5
	$1.00\cdot10^{-1}$	991.90	856.32	91	11.3
		$[C_7mim][Cl]$			
293.2	$1.00\cdot10^{-4}$	998.23	882.41	150	12.3
	$1.00\cdot10^{-3}$	998.23	882.41	146	12.1
	$2.50\cdot10^{-3}$	998.23	882.41	141	11.9
	$5.00\cdot10^{-3}$	998.24	882.41	137	11.7
	$1.00\cdot10^{-2}$	998.24	882.41	133	11.5
	$2.50\cdot10^{-2}$	998.24	882.41	128	11.3
	$5.00\cdot10^{-2}$	998.37	882.41	124	11.1
	$1.00\cdot10^{-1}$	998.42	882.41	119	10.9
298.2	$1.00\cdot10^{-4}$	997.07	877.24	143	12.2
	$1.00\cdot10^{-3}$	997.11	877.24	138	12.0
	$2.50\cdot10^{-3}$	997.24	877.24	133	11.8
	$5.00\cdot10^{-3}$	997.37	877.24	129	11.6
	$1.00\cdot10^{-2}$	997.47	877.24	124	11.4
	$2.50\cdot10^{-2}$	997.68	877.24	120	11.2
	$5.00\cdot10^{-2}$	997.79	877.24	116	11.0
	$1.00\cdot10^{-1}$	997.86	877.24	112	10.8
303.2	$1.00\cdot10^{-4}$	995.08	872.06	136	12.1
	$1.00\cdot10^{-3}$	995.09	872.06	131	11.9
	$2.50\cdot10^{-3}$	995.09	872.06	127	11.7
	$5.00\cdot10^{-3}$	995.21	872.06	122	11.5
	$1.00\cdot10^{-2}$	995.25	872.06	117	11.3
	$2.50\cdot10^{-2}$	995.31	872.06	113	11.1
	$5.00\cdot10^{-2}$	995.36	872.06	98	10.9
	$1.00\cdot10^{-1}$	995.52	872.06	93	10.7

308.2	$1.00\cdot10^{-4}$	994.07	866.85	128	12.0
	$1.00\cdot10^{-3}$	994.07	866.85	123	11.8
T (K)	**C_{IL} (mol·dm^{-3})**	**ρ_w (kg·m^{-3})**	**ρ_o (kg·m^{-3})**	**t (s)**	**γ (mN·m^{-1})**
	$2.50\cdot10^{-3}$	994.13	866.85	118	11.6
	$5.00\cdot10^{-3}$	994.23	866.85	113	11.4
	$1.00\cdot10^{-2}$	994.34	866.85	108	11.2
	$2.50\cdot10^{-2}$	994.44	866.85	103	11.0
	$5.00\cdot10^{-2}$	994.64	866.85	98	10.8
	$1.00\cdot10^{-1}$	994.65	866.85	93	10.6
313.2	$1.00\cdot10^{-4}$	992.08	861.60	120	11.9
	$1.00\cdot10^{-3}$	992.13	861.60	116	11.7
	$2.50\cdot10^{-3}$	992.17	861.60	111	11.5
	$5.00\cdot10^{-3}$	992.18	861.60	106	11.3
	$1.00\cdot10^{-2}$	992.25	861.60	101	11.1
	$2.50\cdot10^{-2}$	992.34	861.60	96	10.9
	$5.00\cdot10^{-2}$	992.41	861.60	91	10.7
	$1.00\cdot10^{-1}$	992.64	861.60	87	10.5
318.2	$1.00\cdot10^{-4}$	991.04	856.33	113	11.8
	$1.00\cdot10^{-3}$	991.04	856.33	108	11.6
	$2.50\cdot10^{-3}$	991.05	856.33	104	11.4
	$5.00\cdot10^{-3}$	991.05	856.33	100	11.2
	$1.00\cdot10^{-2}$	991.05	856.33	96	11.0
	$2.50\cdot10^{-2}$	991.17	856.33	91	10.8
	$5.00\cdot10^{-2}$	991.24	856.33	87	10.6
	$1.00\cdot10^{-1}$	991.31	856.33	82	10.4
		[C_8mim][Cl]			
293.2	$1.00\cdot10^{-4}$	998.23	882.43	137	11.3
	$1.00\cdot10^{-3}$	998.23	882.43	132	11.1
	$2.05\cdot10^{-3}$	998.23	882.43	127	10.9
	$5.00\cdot10^{-3}$	998.24	882.43	122	10.7
	$1.00\cdot10^{-2}$	998.25	882.43	117	10.5
	$2.50\cdot10^{-2}$	998.25	882.43	112	10.3
	$5.00\cdot10^{-2}$	998.39	882.43	107	10.1
	$1.00\cdot10^{-1}$	998.45	882.43	101	9.9
298.2	$1.00\cdot10^{-4}$	997.09	877.25	129	11.2
	$1.00\cdot10^{-3}$	997.15	877.25	124	11.0
	$2.50\cdot10^{-3}$	997.20	877.25	120	10.8
	$5.00\cdot10^{-3}$	997.36	877.25	116	10.6
	$1.00\cdot10^{-2}$	997.44	877.25	111	10.4
	$2.50\cdot10^{-2}$	997.57	877.25	107	10.2
	$5.00\cdot10^{-2}$	997.67	877.25	102	10.0
	$1.00\cdot10^{-1}$	997.77	877.25	97	9.8
303.2	$1.00\cdot10^{-4}$	995.08	872.07	121	11.1

T (K)	C_{IL} (mol·dm^{-3})	ρ_w (kg·m^{-3})	ρ_o (kg·m^{-3})	t (s)	γ (mN·m^{-1})
	$1.00\cdot10^{-3}$	995.09	872.07	117	10.9
	$2.50\cdot10^{-3}$	995.09	872.07	113	10.7
	$5.00\cdot10^{-3}$	995.14	872.07	109	10.5
	$1.00\cdot10^{-2}$	995.28	872.07	104	10.3
	$2.50\cdot10^{-2}$	995.33	872.07	100	10.1
	$5.00\cdot10^{-2}$	995.40	872.07	96	9.9
	$1.00\cdot10^{-1}$	995.54	872.07	91	9.7
308.2	$1.00\cdot10^{-4}$	994.59	866.86	113	11.0
	$1.00\cdot10^{-3}$	994.08	866.86	108	10.8
	$2.50\cdot10^{-3}$	994.24	866.86	104	10.6
	$5.00\cdot10^{-3}$	994.34	866.86	100	10.4
	$1.00\cdot10^{-2}$	994.44	866.86	96	10.2
	$2.50\cdot10^{-2}$	994.54	866.86	91	10.0
	$5.00\cdot10^{-2}$	994.64	866.86	87	9.8
	$1.00\cdot10^{-1}$	994.74	866.86	82	9.6
313.2	$1.00\cdot10^{-4}$	992.18	861.62	105	10.9
	$1.00\cdot10^{-3}$	992.19	861.62	101	10.7
	$2.50\cdot10^{-3}$	992.20	861.62	97	10.5
	$5.00\cdot10^{-3}$	992.31	861.62	92	10.3
	$1.00\cdot10^{-2}$	992.38	861.62	88	10.1
	$2.50\cdot10^{-2}$	992.38	861.62	84	9.9
	$5.00\cdot10^{-2}$	992.44	861.62	80	9.7
	$1.00\cdot10^{-1}$	992.72	861.62	75	9.5
318.2	$1.00\cdot10^{-4}$	991.04	856.35	99	10.8
	$1.00\cdot10^{-3}$	991.04	856.35	95	10.6
	$2.50\cdot10^{-3}$	991.04	856.35	90	10.4
	$5.00\cdot10^{-3}$	991.05	856.35	86	10.2
	$1.00\cdot10^{-2}$	991.05	856.35	82	10.0
	$2.50\cdot10^{-2}$	991.06	856.35	77	9.8
	$5.00\cdot10^{-2}$	991.20	856.35	73	9.6
	$1.00\cdot10^{-1}$	991.92	856.35	69	9.4

[a] The standard uncertainties u are u (C)=0.01×10^{-3}mol·dm^{-3}, u (ρ)=0.01 kg·m^{-3}, u (t)=1 s and u (γ)=0.1 mN·m^{-1}.

References

[1] Sarangi, S. S., Raju, S. G. and Balasubramanian, S., "Molecular dynamics simulations of ionic liquid-vapour interfaces: Effect of cation symmetry on structure at the interface", *Phys. Chem. Chem. Phys*., **13** (7), 2714 (2011).

[2] Dong, B., Li, N., Zheng, L., Yu, L. and Inoue, T., "Surface adsorption and micelle formation of surface active ionic liquids in aqueous solution", *Langmuir*, **23** (8), 4178 (2007).

[3] Ghatee, M. H. and Zolghadr, A. R., "Surface tension measurements of imidazolium-based ionic liquids at liquid-vapor equilibrium", *Fluid Phase Equilib*., **263** (2), 168 (2008).

[4] Azizov, A. H., Aliyeva, R. V., Kalbaliyeva, E. S. and Ibrahimova, M. J., "Selective synthesis and the mechanism of formation of the oligoalkylnaphthenic oils by oligocyclization of 1-hexene in the presence of ionic-liquid catalysts", *Appl. Catal. A: Gen*., **375** (1), 70 (2010).

[5] Likhanova, N. V., Domínguez-Aguilar, M. A., Olivares-Xometl, O., Nava-Entzana, N., Arce, E. and Dorantes, H., "The effect of ionic liquids with imidazolium and pyridinium cations on the corrosion inhibition of mild steel in acidic environment", *Corros. Sci*., **52** (6), 2088 (2010).

[6] Zhou, Z., Jing, G. and Zhou, L., "Characterization and absorption of carbon dioxide into aqueous solution of amino acid ionic liquid [N1111][Gly] and 2-amino-2-methyl-1-propanol", *Chem. Eng. J*., **204**, 235 (2012).

[7] Zhang, X. J., Wang, J. Y. and Hu, Y.Q., "Interfacial tension of n-alkane and ionic liquid systems", *J. Chem. Eng. Data*, **55** (11), 4687 (2010).

[8] Ha, S. H., Mai, N. L. and Koo, Y. M., "Butanol recovery from aqueous solution into ionic liquids by liquid-liquid extraction", *Process Biochem*., **45** (12), 1899 (2010).

[9] Gao, R. and Zheng, J., "Direct electrochemistry of myoglobin based on DNA accumulation on carbon ionic liquid electrode", *Electrochem. Commun*., **11** (7), 1527 (2009).

[10] Li, P., Du, Z., Wang, G., Zhi, L. and Huazhong, S., "Adsorption and aggregation behavior of n-undecyl ammonium acetate ionic liquid in aqueous solution", *J. Disper. Sci. Technol*., **35** (3), 364 (2013).

[11] Qi, X., Zhang, X., Luo, G., Han, C., Liu, C. and Zhang, S., "Mixing behavior of conventional cationic surfactants and ionic liquid surfactant 1-tetradecyl-3-methylimidazolium bromide ([C_{14}mim]Br) in aqueous medium", *J. Disper. Sci. Technol*., **34**, 125 (2012).

[12] Zhao, Y., Yue, X., Wang, X., Huang, D. and Chen, X., "Micelle formation by N-alkyl-N-methylpiperidinium bromide ionic liquids in aqueous solution", *Colloids. Surf. A*, **412**, 90 (2012).

[13] Matsubara, H., Onohara, A., Imai, Y., Shimamoto, K., Takiue, T. and Aratono, M., "Effect of temperature and counterion on adsorption of imidazolium ionic liquids at air-water interface", *Colloids Surf. A*, **370** (1-3), 113 (2010).

[14] Srinivasa Rao, K., Gehlot, P. S., Trivedi, T. J. and Kumar, A., "Self-assembly

of new surface active ionic liquids based on aerosol-OT in aqueous media", *J. Colloid Interface Sci*., **428**, 267 (2014).

[15] Saien, J. and Asadabadi, S., "Temperature effect on adsorption of imidazolium-based ionic liquids at liquid–liquid interface", *Colloids Surf. A*, **431**, 34 (2013).

[16] Misek, T., "Standard Test Systems for Liquid Extraction", Instn. Chem. Engs. for European Federation of Chemical Engineers, Warwickshire, (1985).

[17] Waheed, M. A., Henschke, M. and Pfennig, A., "Mass transfer by free and forced convection from single spherical liquid drops", *Int. J. Heat Mass Transfer*, **45** (22), 4507 (2002).

[18] Saien, J. and Akbari, S., "Variations of interfacial tension of the n-butyl acetate + water system with sodium dodecyl sulfate from (15-22)°C and pH between 6 and 9", *J. Chem. Eng. Data*, **53** (2), 525 (2008).

[19] Bäumler, K., Wegener, M., Paschedag, A. R. and Bänsch, E., "Drop rise velocities and fluid dynamic behavior in standard test systems for liquid/liquid extraction-experimental and numerical investigations", *Chem. Eng. Sci.*, **66** (3), 426 (2011).

[20] Torab-Mostaedi, M., Safdari, J. and Torabi-Hokmabadi, F., "Prediction of mean drop size in pulsed packed extraction columns", *Iran. J. Chem. Eng*. **8** (4), 3 (2011).

[21] Vaghela, N. M., Sastry, N. V. and Aswal, V. K., "Effect of additives on the surface active and morphological features of 1-octyl-3-methylimidazolium halide aggregates in aqueous media", *Colloids Surf. A*, **373** (1-3), 101 (2011).

[22] Huddleston, J. G., Willauer, H. D., Swatloski, R. P., Visser, A. E. and Rogers, R. D., "Room temperature ionic liquids as novel media for 'clean' liquid-liquid extraction", *Chem. Commun*., (16), 1765 (1998).

[23] Lee, B. B., Ravindra, P. and Chan, E. S., "New drop weight analysis for surface tension determination of liquids", *Colloids Surf. A*, **332** (2-3), 112 (2009).

[24] Saien, J., Rezvani Pour, A. and Asadabadi, S., "Interfacial tension of n-hexane-water system under influence of magnetite nanoparticles and sodium dodecyl sulfate assembly at different temperatures", *J. Chem. Eng. Data*, **59** (6), 1835 (2014).

[25] Saien, J. and Asadabadi, S., "Adsorption and interfacial properties of individual and mixtures of cationic/nonionic surfactants in toluene + water chemical systems", *J. Chem. Eng. Data*, **55** (9), 3817 (2010).

[26] Harkins, W. D. and Brown, F. E., "The determination of surface tension (free surface energy), and the weight of falling drops: The surface tension of water and benzene by the capillary height method", *J. Am. Chem. Soc*., **41** (4), 499 (1919).

[27] Bahramian, A. and Danesh, A., "Prediction of liquid-liquid interfacial tension in multi-component systems", *Fluid Phase Equilib*., **221** (1-2), 197 (2004).

[28] Apostoluk, W. and Drzymala, J., "An improved estimation of water–organic liquid interfacial tensions based on linear solvation energy relationship approach", *J. Colloid Interface Sci*., **262** (2), 438 (2003).

[29] Pashley, R. M. and Karaman, M. E., Applied Colloid and Surface Chemistry, Wiley, Hoboken, (2004).

[30] Ríos, H. E., González-Navarrete, J., Vargas, V. and Urzúa, M. D., "Surface properties of cationic polyelectrolytes hydrophobically modified", *Colloids Surf. A*, **384** (1-3), 262 (2011).

[31] Wang, X., Liu, J., Yu, L., Jiao, J., Wang, R. and Sun, L., "Surface adsorption and micelle formation of imidazolium-based zwitterionic surface active ionic liquids in aqueous solution", *J. Colloid Interface Sci*., **391**, 103 (2013).

[32] Markin, V. S., Volkova-Gugeshashvili, M. I. and Volkov, A. G., "Adsorption at liquid interfaces: The generalized Langmuir isotherm and interfacial structure", *J. Phys. Chem. B*, **110** (23), 11415 (2006).

[33] Saien, J. and Akbari, S., "Interfacial tension of hydrocarbon + different pH aqueous phase systems in the presence of Triton X-100", *Ind. Eng. Chem. Res.*, **49** (7), 3228 (2010).

[34] Karakashev, S. I., Nguyen, A. V. and Miller, J.D., "Equilibrium adsorption of surfactants at the gas-liquid interface", *Adv. Polym. Sci*., **218**, 25 (2008).

[35] Chattoraj, D. K. and Birdi, K. S., Adsorption and the Gibbs Surface Excess, Plenum Press, New York, (1984).

[36] Otto, M., Chemometrics: Statistics and Computer Application in Analytical Chemistry, Wiley, New York, (1999).

[37] Erbil, H. Y., Surface Chemistry of Solid and Liquid Interfaces, Blackwell Publishing, Oxford, (2006).

[38] Fainerman, V. B., Mobius, D. and Miller, R., Surfactants: Chemistry, Interfacial Properties, Applications, Elsevier, Amsterdam, (2001).

[39] Radzio, K. and Prochaska, K., "Interfacial activity of trioctyloamine in hydrocarbon/water systems with nonorganic electrolytes", *J. Colloid Interface Sci*., **233** (2), 211 (2001).